INTERACTION LAWS AND THE DETACHMENT EFFECT IN GRANULAR MEDIA

S. LUDING[*/**], E. CLÉMENT[**], A. BLUMEN[*], J. RAJCHENBACH[**], AND J. DURAN[**]
[*] Theoretische Polymerphysik, Universität Freiburg, Rheinstraße 12, D-79104 FREIBURG, GERMANY.
[**] Laboratoire d'Acoustique et d'Optique de la Matière Condensée, Université Pierre et Marie Curie 4, place Jussieu, 75005 PARIS, FRANCE.

Abstract

We study granular materials using both event driven (ED) and molecular dynamics (MD) methods. In the MD simulations we implement linear as well as nonlinear forces and also hysteretic interactions. For multiple collisions the two methods show differences: MD calculations lead to weak, whereas ED methods result in rather strong dissipation, as determined through an effective restitution coefficient.

Introduction and Background

Recent years have seen much effort in understanding granulates, which are assemblies of solid, possibly nonuniform, particles, interacting via contact forces. Summaries of the present knowledge on granular media are given in Refs.[1-2]. These materials display size-segregation, heap formation under vibration and bulk dilatation, as well as density wave formation and 'decompaction' [3]; their fluid-like properties include convection rolls, surface fluidization, and surface waves.

Probing the dynamics of granular particles on scales comparable to their dimensions is difficult. Advances have been made by investigating model systems, such as assemblies of relatively large spheres. Here the binary interactions are quite well understood, both experimentally [4] and theoretically [4,5]; however, multiparticle interactions have been often neglected. Using binary interactions, numerical simulations [6] allow to study the dynamics of many particle systems and by this complement the experimental findings and the analytical approaches [7]; numerically one uses molecular dynamics (MD) [8-10] as well as event-driven (ED) algorithms [11-13].

The MD techniques often involve ad-hoc microscopic assumptions, such as linear [9] or non-linear [10] interactions between the spheres. Evidently the specific contact laws which depict the microscopic situation are fundamental [14,15]; here a major advance are the recently proposed hysteretic interaction laws [14] which lead directly to dissipation. Event-driven (ED) procedures are another means to simulate granulates see e.g. Lubachevsky [11]. Using ED simulations the "cooling" of one-dimensional (1D) granular media was investigated [12] and the ED method was extended to handle the occurrence of connected clusters in 1D [13]. Moreover arrays of spheres under vibration were described using both MD and ED methods [12,13,15,16].

We have shown that MD calculations may display anomalously low energy losses [15], due to the interactions used; the effect may subsist even in the limit of very 'hard' interactions. Then the spheres may separate completely, so that we called the effect "detachment" [15]. Detachment is different from the decompaction evidenced in 2D dissipative granular systems [3]: Decompaction is due to the friction with the walls, whereas detachment follows from the

elastic forces assumed. In fact detachment dissappears in ED simulations.

In this note we report MD simulations using different interactions (linear, non-linear and hysteretic) and compare the results with corresponding ED simulations. The basic difference between ED and MD methods is the contact time t_c. In ED the time t_c in which colliding particles are in contact is ideally zero. This is quite different from MD, for which t_c does not vanish and in fact turns out to be quite significant.

Simulations

We follow the 1D dynamics of a column of N spheres; these are numbered from below starting with $i = 1$. For the immobile bottom plate we set $i = 0$. Due to the 1D aspect, the order of the spheres never changes and we can even dispense with accounting for their diameter d. This fact permits to use diameter-independent coordinates $z_i(t)$; these are related to the diameter dependent coordinates $h_i(t)$ through $z_i(t) = h_i(t) - (i-1)d - d/2$.

We start with a short description of the ED procedures, which follow a sequence of events. Between events Newton's equation of motion for each object is solved analytically. An object is a sphere or the bottom plate; an event is defined for a sphere by a sudden change in momentum, i.e. a collision. Each object i follows its own undisturbed trajectory between events, because dissipation occurs only upon collisions. The times between collisions are determined through a sequential procedure, see Refs.[12,13]. We note that ED simulations take care of the energy loss in collisions through restitution coefficients ε; furthermore, this is the only way energy losses are accounted for. In the center of mass reference frame of two identical colliding particles, the incoming velocities are $+V$ and $-V$ and the outgoing velocities are $-\varepsilon V$ and $+\varepsilon V$. A similar form also holds for collisions with the bottom plate, which is assumed to have infinite mass. Sphere 1 in the reference frame of the plate has a velocity V just before the collision and the velocity $-\varepsilon_p V$ after the collision. A detailed description of the procedure may be found in Refs.[12,13].

Distinct from ED simulations, where one defines a collision matrix in the system's frame of reference, MD calculations are based on elastic and dissipative forces. In our MD procedure we use a fifth order predictor-corrector algorithm [6] for the integration of the equations of motion.

In MD two particles (or a particle and a wall) interact when their relative distance r_{ij}, is smaller than the sum of their radii (the radius of the particle). Here $r_{ij} = \left| \boldsymbol{r}_{ij} \right|$ and $\boldsymbol{r}_{ij}$ points from the center of i to the center of j. In a 1D model only forces in the normal direction, $\boldsymbol{n}_{ij} = \boldsymbol{r}_{ij}/r_{ij}$ matter. Thus two forces are active in the regime $d > r_{ij}$; first, an elastic restoration force:

$$f_{el}^{(i)} = -Kx^{1+\beta} \tag{1}$$

where K is the spring constant and x is the (positive) penetration depth $x = d - r_{ij}$. Second, a frictional force in the normal direction:

$$f_n^{(i)} = -D_n m_n \left[\boldsymbol{v}_{ij} \cdot \boldsymbol{n}_{ij} \right] x^\gamma \tag{2}$$

where $\boldsymbol{v}_{ij}$ is the relative velocity of particles i and j, D_n is the normal dissipation parameter and the normalized mass is $m_n = 2m_{red} = 2m_i m_j / (m_i + m_j)$. The parameters β and γ fix the non-

linearity of the forces; thus $\beta = \gamma = 0$ leads to a linear spring-dashpot (LSD) interaction. From Eqs.(1) and (2) and for LSD the contact time $t_c = \pi\big/\sqrt{K/m_{\text{red}} - D_n^2}$ and the restitution coefficient $\varepsilon = \exp(-D_n t_c)$ follow, see Ref.[15]. Note that for LSD interactions t_c and ε are velocity independent.

Non-linear forces offer a more general way to mimic collisions. Thus Hertz' model for the interaction of two spheres [5] corresponds to $\beta = 1/2$. For non-linear forces the contact time and the restitution coefficient become velocity dependent, see Ref.[15] for details.

An alternative way to introduce dissipation is to use different forces for loading and unloading [14]. In detail, we use a spring constant K_1 for loading and a larger spring constant K_2 for unloading:

$$f_{\text{el}}^{(i)} = \begin{cases} -K_1 x & \text{for loading} \\ -K_2(x - x_0) & \text{for unloading} \end{cases} \tag{3}$$

This behavior models energy loss due to plastic deformation, with the penetration depth x and a finite penetration $x_0 = (1\text{-}\varepsilon^2)x_{\text{max}}$ at which the contact force vanishes during unloading. $\varepsilon = \sqrt{K_1/K_2}$ is the momentum restitution coefficient and x_0 is defined through the continuity of the forces at maximum penetration, i.e. $K_1 x_{\text{max}} = K_2(x_{\text{max}}\text{-}x_0)$. In Fig.1 we give a schematic plot of the elastic force during the contact of two spheres. During loading the force increases linearly with slope K_1 as a function of x until x_{max} is reached. Unloading follows the larger slope, i.e. K_2, until the force equals zero at a finite penetration x_0. We define the contact time t_c to be the time when the force vanishes, i.e. the time at which again $x = x_0$. When no additional force is active, the penetration decreases and the spheres separate after a time $x_0/v(t_c)$, where $v(t_c)$ is the velocity at time t_c. If for example another sphere hits one of the two original spheres, reloading for $0 < x' < x_0$ may take place with a force $K_2(x\text{-}x')$ until the original loading curve is reached; further reloading follows then the original loading curve. However, this is not the only way to model plastic deformation, see Ref. [14] for extensive details. For the simple hysteretic force, Eq.(3), t_c and ε can be computed [14]; in implicit form one has $K_1 = m_{\text{red}}\pi^2(1+\varepsilon)^2\big/\left(4t_c^2\right)$ and $K_2 = K_1\big/\varepsilon^2$.
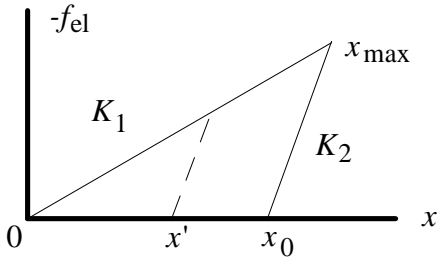

Fig.1:
The elastic force, Eq.(3), plotted as a function of the penetration x. On contact two spheres load from 0 to x_{max} and then unload to x_0. Reloading may take place from x' to the original loading curve.

Multiparticle collisions

We are now interested in the behavior of a column of spheres in 1D. We neglect gravitational effects and analyze the collision of the column with a static boundary. This situation is interesting, since it allows us to compare the MD results, obtained using different interactions, with those obtained by ED methods [12,13].

We introduce the effective restitution coefficient for many particle collisions through $\varepsilon_{\text{eff}} = \sqrt{E_f/E_0}$, where E_0 and E_f denote the kinetic energies of the particles relative to the

bottom plate before and after the collision, respectively, i.e. $E = \frac{m}{2}\sum_{i=1}^{N} v_i^2$.

In Fig.2 we display ε_{eff} obtained from MD and ED simulations. The results depend on the initial separation s_0 between the spheres, the initial velocity v_0 and the contact time t_c. We rescale the axes so that the ratio of the mean time beween events s_0/v_0 to the contact time t_c shows up, i.e. we plot ε_{eff} vs. $\sigma = s_0/(v_0 t_c)$. In Fig.2 we have $N = 10$, $\varepsilon = 0.9$, $t_c = 8.4 \times 10^{-6}$s, and as the initial velocity $v_0 = 0.5$ m/s; furthermore, s_0 varies between 10^{-9} and 3.2×10^{-3}m. In Fig.2 we find that the results of the linear spring-dashpot interaction (LSD) and of the hysteretic interaction model (HYS) agree qualitatively. Two features are proeminent: first, when $\sigma \ll 1$ the energy loss is small, i.e. $\varepsilon < \varepsilon_{eff} \cong 1$ for LSD and $\varepsilon_{eff} \cong \varepsilon$ for HYS. This fact leads to large interparticle distances after the collision with the bottom plate, a phenomenon which we call detachment. Second, for $\sigma \gg 1$ the ε values are lower and the energy loss turns out to be independent of σ [right side of Fig.2]. We note that the ED procedure [the dashed line in Fig.2] leads to $\varepsilon_{eff} \cong 0.341 \pm 0.002$, a result practically independent of s_0 and v_0. While for $\sigma \gg 1$, the ED and MD results agree with each other, there are large differences for $\sigma \ll 1$.
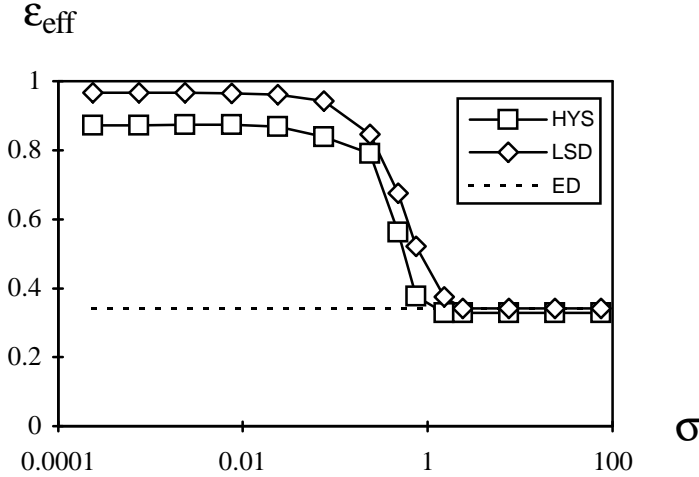

Fig.2:
Linear-logarithmic plot of the effective restitution coefficient ε_{eff} as a function of $\sigma = s_0/v_0 t_c$ for different interaction models, see text for details. The calculations involve $N = 10$ particles with $\varepsilon = 0.9$, colliding with a fixed boundary.

Now we study the dependence of ε_{eff} on the number of particles which hit the wall. In Fig.3 we plot ε_{eff} as a function of N for $s_0 = 0$, $v_0 = 0.5$ ms^{-1}, $d = 1$ mm and for different interaction laws.
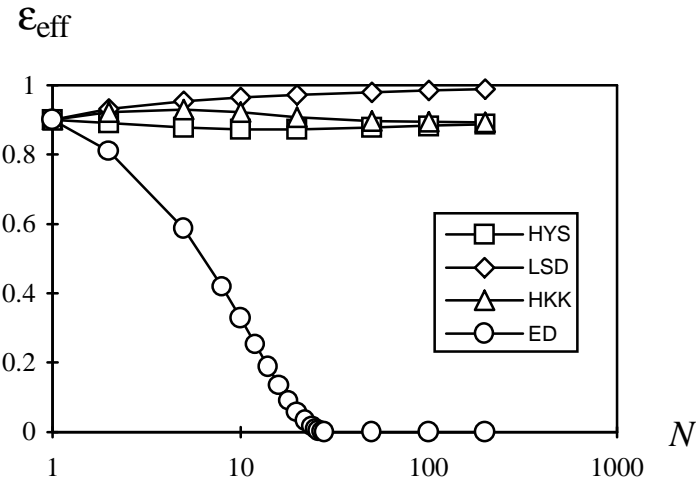

Fig.3:
The effective restitution coefficient ε_{eff}, plotted as a function of N for $s_0 = 0$ and $v_0 = 0.5$ m/s. We use the Hooke interaction ($\beta = \gamma = 0$, LSD), the Hertz-Kuwabara-Kono interaction ($\beta = \gamma = 1/2$, HKK), the hysteretic interaction Eq.(3) (HYS) and the ED method, see text for details.

Using the linear interaction law with $\beta = \gamma = 0$, $K/m_{red} = 8\times10^{10}$ s^{-2}, and $D_n = 9.48\times10^3$ s^{-1} we find that ε_{eff} increases with N. Using the Hertz-Kuwabara-Kono (HKK) interaction, i.e. $\beta = \gamma = 1/2$, with $K/m_{red} = 2\times10^{12}$ s^{-2} m$^{-1/2}$, and $D_n = 3.5\times10^4$ s^{-1} m$^{-1/2}$ we find that ε_{eff} varies little as a function of N. A hysteretic interaction with $K_1/m_{red} = 1.78\times10^{11}$ s^{-2}, and $K_2/m_{red} = 2.2\times10^{11}$ s^{-2}, agrees rather well with ε_{eff} found using the HKK ($\beta = \gamma = 1/2$) law. The detachment effect is weaker for non-linear interactions or for hysteretic interactions when compared to the simple LSD model; nonetheless all ε_{eff} MD results differ from the ED ones, for which ε_{eff} is close to zero for $N(1-\varepsilon)$ large [13].

The difference between ED and MD results is also apparent from the *relative* kinetic energy E_{rel}, also called 'granular temperature' [7]; E_{rel} is defined through $E_{rel} = \frac{m}{2}\sum_{i=1}^{N}(v_i - v_{cm})^2$ where v_{cm} is the velocity of the center of mass of the assembly of spheres.

In Fig.4 we plot $1\text{-}E_{rel}/E_f$ where E_{rel} is the relative energy and E_f is the kinetic energy after collision. The parameters of the simulations are the same as the ones used in Fig.3.
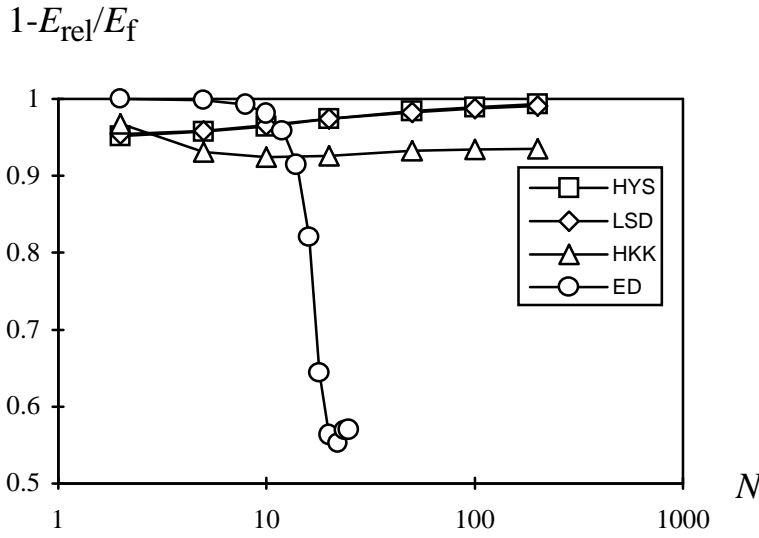
$1\text{-}E_{rel}/E_f$

Fig.4:
$1\text{-}E_{rel}/E_f$ plotted as a function of N. The parameters are as in Fig.3.

Discussion and Conclusions

For MD simulations we introduced various microscopic interaction laws and compared the results with the outcome of ED simulations. The basic difference between ED and MD methods is the time t_c, during which particles are in contact. In ED t_c is implicitly zero, whereas for MD t_c depends on the interaction laws and parameters used. Thus a large spring constant leads, in general, to a small t_c. We found that MD calculations underestimate the energy dissipation when the number of spheres in contact is large. The effect is most obvious for linear interactions but also holds for non-linear interactions and for hysteretic models. Even in the case of very high dissipation, i.e. $N = 10$ and $\varepsilon = 0.6$, detachment occurs in MD calculations, whereas ED simulations lead to an ε_{eff} which virtually vanishes, i.e. to a clustered column after collision.

The occurence of an anomalously low energy dissipation in MD depends on the ratio σ between the time of free flight and t_c. MD simulations underestimate the energy dissipation and lead to large fluctuations for $\sigma \ll 1$. On the other hand, we find that for $\sigma \gg 1$ the results of MD and ED simulations agree with each other.

We close this work on a cautionary note about computer simulations: a careful comparison

of the numerical outcome with experimental benchmarks, as well as a critical evaluation of the parameters used in simulations is required. From our side we view the question of the validity of the simulation methods and of the relevance of the interactions used as being still open in the case of multiparticle contacts.

References

1. *Disorder and Granular Media*, D. Bideau and A. Hansen eds., (Elsevier Sci. Publ., Amsterdam 1993).
2. H. M. Jaeger, S. R. Nagel, Science **255**, 1523 (1992); H. M. Jaeger, J. B. Knight, C.-h. Liu, S. R. Nagel, MRS Bulletin, Vol. XIX, No.5, 25 (1994).
3. J. Duran, T. Mazozi, E. Clément, J. Rajchenbach, (to be published in Phys. Rev. E, 1994).
4. S. F. Foerster, M. Y. Louge, H. Chang, and K. Allia, Phys. Fluids **6**, 1108 (1994).
5. L. D. Landau, E. M. Lifschitz, *Band VII Elastizitätstheorie* (Akademie Verlag, Berlin, 1989); W. Goldsmith, *IMPACT The Theory and Physical Behaviour of Colliding Solids*, (Edward Arnold, Publishers, London, 1964); G. Kuwabara and K. Kono, Jpn. J. Appl. Phys. **26**, 1230 (1987).
6. M. P. Allen and D. J. Tildesley, *Computer Simulation of Liquids* (Oxford University Press, Oxford, 1987).
7. S. B. Savage, J. Fluid Mech. **92**, 53 (1979);
8. P. A. Cundall and O. D. L. Strack, Geotechnique **29**, 47 (1979).
9. J. A. C. Gallas, H. J. Herrmann, S. Sokolowski, Phys. Rev. Lett. **69**, 1371 (1992); Yi Zhang and C. S. Campbell, J. Fluid Mech. **237**, 541 (1992); D. C. Hong, J. A. McLennan, Physica A **187**, 159 (1992); Y-h. Taguchi, Phys. Rev. Lett. **69**, 1367 (1992).
10. G. H. Ristow, Intern. J. Modern Phys. C **3**, 1281 (1993); J. Lee, J. Phys. A **27**, L257 (1994).
11. B. D. Lubachevsky, J. Comput. Phys. **94**, 255 (1991).
12. B. Bernu and R. Mazighi, J. Phys. A **23**, 5745 (1990); S. McNamara, W. R. Young, Phys. Fluids A **4**, 496 (1992); S. McNamara, W. R. Young, Phys. Fluids A **5**, 34 (1993); R. Mazighi, B. Bernu, and F. Deylon, (to be published in Phys. Rev. E, 1994).
13. E. Clément, S. Luding, A. Blumen, J. Rajchenbach and J. Duran, Internat. J. Modern Phys. B **7**, 1807 (1993); S. Luding, E. Clément, A. Blumen, J. Rajchenbach and J. Duran, Phys Rev E **49**, 1634 (1994).
14. M. H. Sadd, Q. Tai, A. Shukla, Intern. J. Non-Lin. Mech. **28**, 251 (1993); C. Y. Zhu, A. Shukla, M. H. Sadd, J. Appl. Mech. **58**, 341 (1991); O. R. Walton, Acta Mechanica **63**, 947 (1986). O. R. Walton, R. L. Braun, J. Rheology **30**, 949 (1986).
15. S. Luding, E. Clément, A. Blumen, J. Rajchenbach and J. Duran, (to be published, Phys. Rev. E, Nov. 1994); S. Luding, E. Clément, A. Blumen, J. Rajchenbach and J. Duran, Phys. Rev. E **50**, R1762 (1994).
16. S. Luding, H. J. Herrmann, and A. Blumen, Phys. Rev. E **50**, 3100 (1994).